Augmented sensitivity of an IR-absorption gas sensor employing a metal hole array

Yoshiaki Nishijima,[1,*] **Yuta Adachi,**[1] **Lorenzo Rosa,**[2,3] **and Saulius Juodkazis**[2,3,4]

[1]*Department of Electrical and Computer Engineering, Graduate School of Engineering, Yokohama National University, 79-5 Tokiwadai, Hodogaya-ku, Yokohama 240-8501, Japan*
[2]*Centre for Micro-Photonics, Faculty of Engineering and Industrial Sciences, Swinburne University of Technology, Hawthorn, VIC 3122, Australia*
[3]*The Australian National Fabrication Facility - ANFF, Victoria node, Faculty of Engineering and Industrial Sciences, Swinburne University of Technology, Hawthorn, VIC, 3122, Australia*
[4]*sjuodkazis@swin.edu.au*
[*]*nishijima@ynu.ac.jp*

Abstract: We demonstrate the use of plasmonic extraordinary transmission at IR wavelengths for surface-enhanced infrared absorption (SEIRA) spectroscopy in gas sensing. Gas detection was performed through non-dispersive infrared (NDIR) absorption. The sensitivity of SF_6 gas detection is increased around $\sim$27 times with metal hole array (MHA) microstructures placed on the gas cell mirrors, as compared with non-structured mirrors; an absorption change of 2% per 100 ppm was obtained on a standard commercial pyroelectric detector. Down-sizing of IR-sensors to a sub-1 mm gas cell width, delivering $\sim$ 40 nM (or 1 ppm) of SF_6 sensitivity, can be foreseen with a simple source-detector setup.

OCIS codes: (240.6680) Surface plasmons; (240.6490) Spectroscopy, surface; (300.6270) Spectroscopy, far infrared.

References and links

1. S. Kumar, J. Huang, J. R. Cushnir, P. Spanel, D. Smith, and G. B. Hanna, "Selected ion flow tube-MS analysis of headspace vapor from gastric content for the diagnosis of gastro-exophageal cancer," Anal. Chem. **84**, 9550–9557 (2012).
2. M. Ueda, N. Teshima, and T. Sakai, "Development of formaldehyde standard gas generator based on gravitational dispensing-vaporization and its application to breath formaldehyde determination," Bunseki Kagaku **57**, 605–612 (2008).
3. M. Zhang, H. C. Su, Y. Rheem, C. M. Hangarter, and N. V. Myung, "A rapid room-temperature NO_2 sensor based on tellurium-SWNT hybrid nanostructures," J. Phys. Chem. C **116**, 20067–20074 (2012).
4. J. Hodgkinson, R. Smith, W. O. Hob, J. R. Saffell, and R. Tatam, "A low cost, optically efficient carbon dioxide sensor based on nondispersive infra-red (NDIR) measurement at 4.2 mm," Proc. SPIE **8439**, 843919 (2012).
5. N. Ohta, K. Nomura, and I. Yagi, "Electrochemical modification of surface morphology of Au/Ti bilayer films deposited on a Si prism for in situ surface-enhanced infrared absorption (SEIRA) spectroscopy," Langmuir **26**, 18097–18104 (2010).
6. H. Miyatake, E. Hosono, M. Osawa, and T. Okada, "Surface-enhanced infrared absorption spectroscopy using chemically deposited Pd thin film electrodes," Chem. Phys. Lett. **428**, 451–456 (2006).
7. H. Aouani, H. Sipova, M. Rahmani, M. Navarro-Cia, K. Hegnerova, J. Homola, M. Hong, and S. A. Maier, "Ultrasensitive broadband probing of molecular vibrational modes with multifrequency optical antennas," ACS Nano **1**, 669–675 (2013).
8. Y. Nishijima, H. Nigorinuma, L. Rosa, and S. Juodkazis, "Selective enhancement of infrared absorption with metal hole arrays," Opt. Mater. Express **2**, 1367–1377 (2012).

#187633 - $15.00 USD Received 25 Mar 2013; revised 26 May 2013; accepted 29 May 2013; published 13 Jun 2013

9. T. W. Ebbesen, H. J. Lezec, H. F. Ghaemi, T. Thio, and P. A. Wolff, "Extraordinary optical transmission through sub-wavelength hole arrays," Nature **351**, 667–669 (1998).
10. C. Genet and T. W. Ebbesen, "Light in tiny holes," Nature **445**, 39–46 (2007).
11. E. Popov, M. Neviere, S. Enoch, and R. Reinisc, "Theory of light transmission through subwavelength periodic hole arrays," Phys. Rev. B **62**, 16100–16108 (2000).
12. T. Rindzevicius, Y. Alaverdyan, A. Dahlin, F. Hook, D. S. Sutherland, and M. Kall, "Plasmonic sensing characteristics of single nanometric holes," Nano Lett. **5**, 2335–2339 (2005).
13. A. Degiron, H. J. Lezec, N. Yamamoto, and T. W. Ebbesen, "Optical transmission properties of a single subwavelength aperture in a real metal," Opt. Commun. **239**, 61–66 (2004).
14. H. Rigneault, J. Capoulade, J. Dintinger, J. Wegner, N. Bonod, E. Popov, T. W. Ebbesen, and P. F. Lenne, "Enhancement of single-molecule fluorescence detection in subwavelength apertures," Phys. Rev. Lett. **95**, 117401 (2005).
15. J. G. Rivas, C. Schotsch, P. H. Bolivar, and H. Kurz, "Enhanced transmission of THz radiation through subwavelength holes," Phys. Rev. B **68**, 201306 (2003).
16. P. Forster, V. Ramaswamy, P. Artaxo, T. Berntsen, R. Betts, D. W. Fahey, J. Haywood, J. Lean, D. C. Lowe, G. Myhre, J. Nganga, R. Prinn, G. Raga, M. Schltz, and R. Van Dorland, "Changes in atmospheric constituents and in radiative forcing," in *Climate Change 2007: The Physical Science Basis. Contribution of Working Group I to the 4th Assessment Report of the Intergovernmental Panel on Climate Change* (Cambridge University Press, 2007).
17. T. Thio, H. F. Ghaemi, H. J. Lezec, P. A. Wolff, and T. W. Ebbesen, "Surface-plasmon-enhanced transmission through hole arrays in Cr films," J. Opt. Soc. Am. B **16**, 1743–1748 (1999).
18. G. Gervinskas, D. Day, and S. Juodkazis, "High-precision interferometric monitoring of polymer swelling using a simple optofluidic sensor," Sens. Actuators B **159**, 39–43 (2011).
19. M. L. Kurth and D. K. Gramotnev, "Nanofluidic delivery of molecules: integrated plasmonic sensing with nanoholes," Microfluid. Nanofluid. **14**, 743–751 (2013).
20. A. Chou, E. Jaatinen, R. Buividas, G. Seniutinas, S. Juodkazis, E. L. Izake, and P. M. Fredericks, "SERS substrate for detection of explosives," Nanoscale **4**, 7419–7424 (2012).

1. Introduction

Gas detection is an important field of analytical chemistry, where high sensitivity and selectivity are sought after for qualitative and quantitative analysis. In the field of medical gas sensing from exhalation, bio-markers of disease can be detected without any medical intervention [1, 2]. In case of environmental sensing in landfills, detection of greenhouse effect gases, exhaust fumes from cars, monitoring of industrial processes, the gases concentration should be monitored continuously in real time with 1 ppm precision or better [3]. The non-dispersive infrared (NDIR) absorption method is widely used for gas sensing, because of its simplicity and high sensitivity [4]. NDIR is based on the single-wavelength detection of a molecular vibrational mode; however, because of the small extinction cross-sections of these modes, a long optical path (in a gas cell) is required, and sensors become relatively large or require optical folding of the light path. We have already demonstrated surface-enhanced infrared absorption (SEIRA [5–7]) with metal hole array (MHA) micro-structures for azo-benzene sensing by spin-coating of the analyte [8]. A strong absorption enhancement appeared on the transmission peaks, and the effective molecular absorption cross-section was increased approximately $10\times$, due to the electromagnetic field enhancement at the rim of the MHA holes in a spectrally narrow window of 10-20 cm^{-1} bandpass. An even higher sensitivity would be expected in the case of gas sensing on a non-specific metal surface where chemosorption is not taking place. This was predicted by simulations [8] showing that up to $40\times$ enhancement exists inside the MHA holes at the Si-Ag interface, and constitutes the IR version of the extraordinary transmission demonstrated at visible wavelengths [9–15].

In this study, we demonstrate the application of MHAs to gas sensing of a single-wavelength signature vibration mode. The SF_6 gas, which has one of the most powerful green house effects, and is heavily used in Si processing including solar cells, was chosen for this study (its 100-year impact in terms of global warming potential, using CO_2 as a reference, is 22800, as compared with methane at 25 and water at 298 [16]). The light source and detector are comparatively

#187633 - $15.00 USD Received 25 Mar 2013; revised 26 May 2013; accepted 29 May 2013; published 13 Jun 2013

inexpensive standard commercial devices already designed for SF_6 monitoring; we use them together with our custom-designed gas cell, whose windows were made from Si plates carrying MHAs.

2. Experimental

The fabrication of the designed MHA, having nano-to-micro-sized holes with specific spatial arrangement, has been carried out via standard lithography and lift-off processing [8]. The structures were defined by standard contact photolithography using mask projection. A low-dopant silicon substrate (Global Top Chemical Co. Ltd.) with both side polished was coated by COAT200 (Tokyo Ohka Kogyo Co. Ltd.) to obtain a hydrophobic surface. Then, a positive type photo-resist (OFPR-500, Tokyo Ohka Kogyo Co. Ltd.) was spin-coated at 3000 rpm for 60 s and prebaked at 90°C for 90 s. The contact photomask exposure was implemented with UV light using a mask aligner (MA-10, MIKASA Co. Ltd.). A substrate area of 2×2 cm^2 was used for pattern fabrication, and the mask area was over 5×5 cm^2; therefore, a homogeneous pattern was prepared on the whole substrate area. The series of hole diameter c and period a combinations are designed as (c, a) = (1.4, 2.9), (1.5, 3.1), (1.6, 3.3), (1.7, 3.5), (1.8, 3.7), (1.9, 3.9), (2.1, 4.2), and (2.3, 4.6) μm, respectively. Due to the resolution of photomask preparation, we have $a = 2c$ or slightly larger than $2c$. After exposure, the samples were developed in 2.38% tetramethyl ammonium hydroxide (NMD-3, Tokyo Ohka Kogyo Co. Ltd.), dried, and coated with a 3 nm Ni adhesion layer followed by a 50 nm Ag layer using vapor deposition. The following lift-off step in acetone under ultrasonic bath conditions removed the resist together with the excess metal, and finally the sample was washed in methanol.

Optical transmission of the MHAs was measured with a Fourier-transform IR spectrometer (FTIR-6200 JASCO Co. Ltd.). Gas sensor detection measurements were performed with a self-developed non-dispersive infrared (NDIR) measurement system. Figure 1 shows the outline of

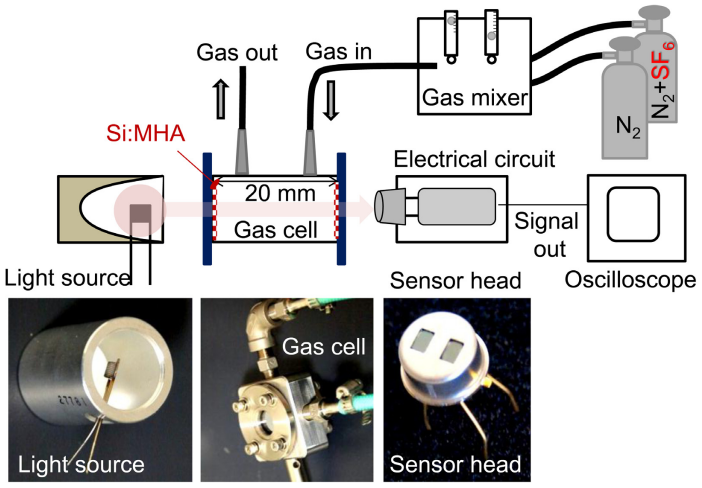

Fig. 1. Schematic illustration of the SF_6 gas detection set up used in the experiments. The IR light source is a IRS-001C (IRS, Ltd.) and the SF_6 detector is a LIM-122 (Infratec, LLC). The gas cell mirrors were replaced with Si substrates carrying silver multi hole arrays (MHA) for augmented sensitivity. Size reference: the output diameter of the parabolic mirror is ~ 2.5 cm, the window diameter of the gas cell is 1.5 cm, and a single window on the detector cap measures 3.5×2.5 mm^2.

#187633 - $15.00 USD Received 25 Mar 2013; revised 26 May 2013; accepted 29 May 2013; published 13 Jun 2013

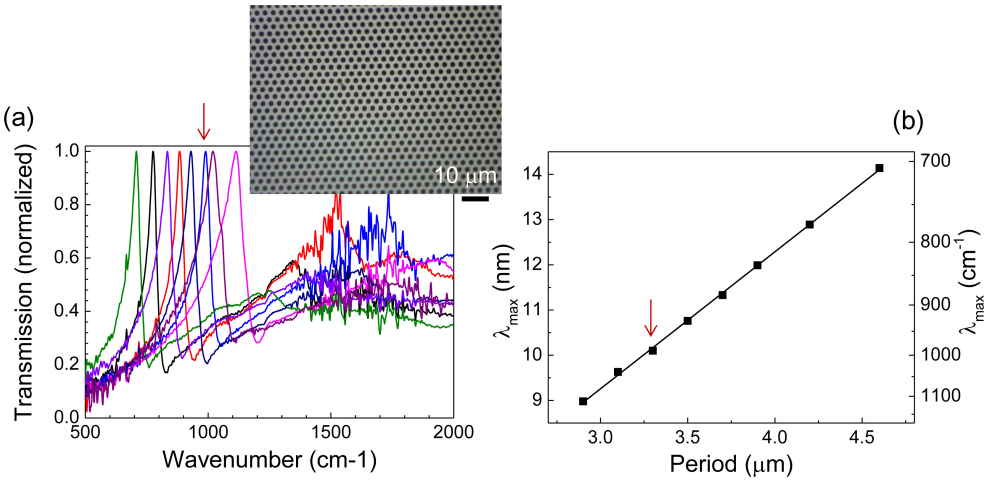

Fig. 2. (a) Normalized optical transmission of the silver hexagonal MHAs with hole diameters / periods (c, a), measured right-to-left in μm: (1.4, 2.9), (1.5, 3.1), (1.6, 3.3), (1.7, 3.5), (1.8, 3.7), (1.9, 3.9), (2.1, 4.2), and (2.3, 4.6). The inset shows the optical micro-photograph of the fabricated MHA with $(c,a) = (1.6, 3.3)$. (b) Plot of the peak wavelength as a function of the period a. The arrows mark the MHA used for SF_6 detection at 950 cm^{-1}, which is shown in the inset of the (a) panel.

the experimental setup. A filament-type infrared light source (IRS-001C, IRS Co.) was used to deliver black-body-like emission with an applied voltage of 4.5 V. No special IR optics was used; the IR emission was collected by a parabolic back-reflector with a $\sim 7^{\circ}$ divergence, and then used to illuminate the 1.5 cm diameter gas cell window, whose output illuminated the 3.5×2.5 mm^2 filter window of the detector, having an active detecting area of 1.8×1 mm^2. The radiation was transmitted into the gas cell through two replaceable windows, which permitted to exchange the Si mirrors with Si:MHA mirrors. Then, a specific-designed pyroelectric sensor (LIM-122, Infratec Ltd.) was used for detection of the SF_6 vibration bands, by monitoring two bands around the wavelengths of 8.26 μm (reference) and 10.6 μm or 943 cm^{-1} (signature signal for SF_6). The gas concentration was controlled by a mixing system shown in Fig. 1. A concentration of 100 ppm of SF_6 in N_2 carrier gas was progressively diluted by pure N_2 (99.99% purity), and the mixing ratio was controlled through a flow meter. The detector output signal was detected on an oscilloscope.

3. Simulations

The transmission and field enhancement properties of the gas cell realized with Si:MHA mirrors at both ends have been simulated with a 3D finite-difference time-domain (3D-FDTD) model implemented with the Lumerical software from FDTD Solutions. Due to the complexity of the model, the simulations were performed on the swinSTAR supercomputer at Swinburne University, featuring 16-core computational nodes with 64 GB memory each. The memory footprint of each simulation was around 100 GB and took from 1 to 3 hours running on a 16-node cluster.

#187633 - $15.00 USD Received 25 Mar 2013; revised 26 May 2013; accepted 29 May 2013; published 13 Jun 2013

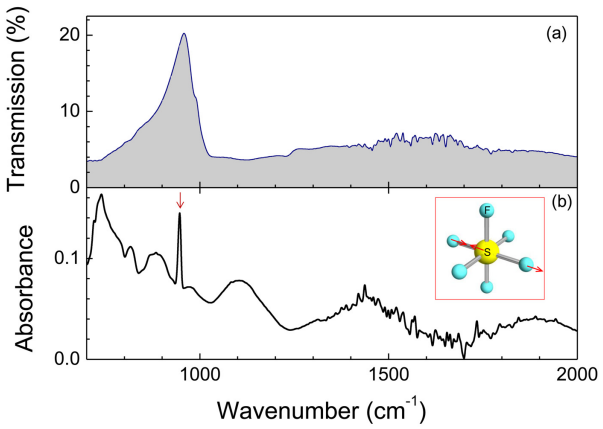

Fig. 3. (a) Transmission spectra of gas cell with two Si:MHA windows filled with air (transmission of single MHA was up to 40%). (b) SF_6 gas absorption spectrum measured in a gas cell filled with SF_6. The inset shows the asymmetric stretching mode of the SF_6 molecule; the corresponding band at 943 cm^{-1} is pointed at by an arrow in panel (b).

4. Results and Discussion

4.1. Transmission spectra of MHA

Figure 2 shows the optical characterization of the hexagonal-lattice MHA, which was fabricated in homogeneous uniform structures over a 2×2 cm^2 area. The transmission spectra of hexagonal-lattice MHAs is similar to that of the square lattice, except for the fact that the hexagonal pattern shows a single transmission peak. The absolute transmission value is larger than that of a square pattern by $\sim 40\%$ for a 50 nm Ag thickness, as compared with ~ 20 nm of square-lattice thickness; hence, more mirrors can be lined up for increased selectivity, while obtaining the same detection threshold. The transmission peak is red-shifted with increasing pattern period a, following a linear dependence (Fig. 2(b)). The peak wavelength of MHA transmission is given by the following equation [17]:

$$\lambda_{\max} = \frac{\sqrt{3}}{2} \frac{a}{\sqrt{i^2 + ij + j^2}} \cdot \sqrt{\frac{\varepsilon_1 \varepsilon_2}{\varepsilon_1 + \varepsilon_2}}, \tag{1}$$

where $\varepsilon_{1,2}$ are the dielectric constants of the metal (e.g. $\varepsilon_1 = -2700 + 1400\mathrm{i}$ for Ag at 10 μm wavelength) and the surrounding media ($\varepsilon_2 \simeq 11.7 + 5 \times 10^{-4}\mathrm{i}$ for Si), respectively; and i and j are the MHA diffraction orders in the two principal directions of the hexagonal lattice (x-direction and 60°-angled direction, in this case). The transmission peak appearing in Fig. 2(a) is characterized as the $(i = 1, j = 0)$, or $(i = 0, j = 1)$ peak. The second-order peak $(i = 1, j = 1)$ should appear at a $1/\sqrt{3}$ times shorter wavelength according to Eq. (1), however we could not see it experimentally. This might be due to the weak strength of second-order diffractions.

Experimental results (Fig. 2(b)) well agree with this equation. The vibrational mode of the SF_6 gas is well known, showing as a 10.6 μm (943 cm^{-1}) band which can be assigned to the asymmetric stretching of the F-S-F covalent bond. Therefore, according to this relationship between the periodicity and the peak transmission wavelength, we choose a period $a = 3.3$ μm for the SEIRA gas sensor.

Figure 3 shows the transmission spectra of a gas cell with both mirrors carrying MHA patterns. The peak transmission obtained has an absolute value around 20%. The peak is centered

#187633 - $15.00 USD Received 25 Mar 2013; revised 26 May 2013; accepted 29 May 2013; published 13 Jun 2013

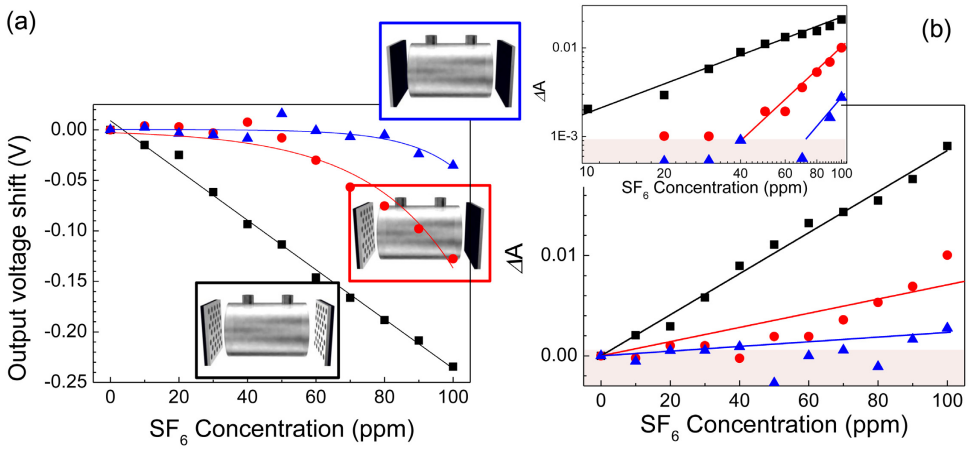

Fig. 4. (a) Output signal dependence on the SF6 concentration. The insets show schematically the configuration of the gas cell windows (whether the MHA is exposed to the inside of the gas cell or not). (b) Absorption change $\Delta A = -\log(I/I_0)$ as a function of SF_6 concentration; the hashed region marks the detection threshold at $\sim 0.1\%$. The line is the linear fitting by the least-squares method. The inset figure shows the log-log plot of absorption and concentrations. The lines are drawn as eye guides for the linear dependence.

around 950 cm^{-1} and is well-matched with the SF_6 signature absorption peak.

In actual gas sensing experiments (Fig. 4), we used three different window configurations for comparison. We have windows on both sides of the gas cell, as shown in Fig. 1. Firstly, both MHA patterns were located on the inward wall of the window (exposed to SF_6, black-framed picture inset in Fig. 4(a)). Secondly, one MHA mirror was flipped over with bare Si facing the gas cell interior red-framed; in the third configuration, both MHAs were facing outside the cell (blue-framed). If the MHAs played an important role for SF_6 detection sensitivity, these three configurations would allow to see a difference. Also, since we always had MHAs on the windows, the absolute transmittance was almost constant in all three cases.

The output signal dependence vs. the gas concentration is shown in Fig. 4. When the MHAs were placed to face outside the gas cell, the output signal started decreasing at around 80 ppm (which is almost the same result as when two silicon substrates without MHA were used as windows, blue plot). However, for both MHAs facing inside the gas cell (black plot), the absorption change (decrease of signal) started at around 5 ppm (10 ppm corresponds to 400 nM concentration in normal conditions: 1 atm pressure at 20°C temperature). With one MHA inwards and the other outward-looking, the change of detected signal started at 50 ppm (red plot). This is almost half-way between the threshold sensitivities, as would be expected with MHAs playing a role in enhancement of absorption via the SEIRA mechanism. For the quantification of effect, the absorption calculated as $A = -\log(I/I_0)$ (I is the detected signal), with I_0 defined at 0 ppm, was plotted as a function of the concentration of SF_6 (Fig. 4(b)). According to the Lambert-Beer law, concentration of the SF_6 is in linear relationship to the absorbance change (ΔA). The slope of $\Delta A/\Delta[SF_6]$, which is connected to the enhancement absorption cross-section, was increased 27 times when both mirrors had inward MHAs (and 9 times for one-sided inward MHA). When two MHA patterns were facing the interior of the gas cell, the dependence (shown in the inset of panel (b)) was linear in a log-log plot, and super-linear in the other two cases where one or none of the MHAs were exposed to SF_6. This indicates that the bulk absorption of the 2-cm-long cell was significant for the latter cases.

#187633 - $15.00 USD Received 25 Mar 2013; revised 26 May 2013; accepted 29 May 2013; published 13 Jun 2013

Gas sensing on the surface of MHA due to electromagnetic field enhancement is consistent with our previous study [8]. The observed enhancement is due to the optical near-field effect on the MHAs and the spacing between two MHAs substrates is not fully optimized. Only the SF_6 molecules in close proximity of the MHA experience field enhancement due to plasmon resonance and extraordinary transmission. The field enhancement effective for SEIRA gas detection will be discussed the next section. Also, the transport efficiency of the target molecules to the enhancement field region is important for sensing stability and time cost. The mean free path of molecules in air at atmospheric pressure can be estimated as $l_f = (\sqrt{2}\pi n a_N^2)^{-1} = 60$ nm for the N_2 molecule of size $a_N = 0.3$ nm and density $n = 2.69 \times 10^{19}$ cm^{-3} at room temperature $T = 300$ K. The diffusion coefficient $D = \frac{1}{3} l_f v_T = 10^{-5}$ m^2/s, where $v_T \simeq 0.5$ km/s is the velocity of molecules in air at room temperature $T = 300$ K. The measurements were carried out on a time interval $t_m = 5$ min to obtain a reliable readout signal (about 10 s is required to observe a change in the readout signal); hence, the diffusion length of the molecules is $L_d = \sqrt{Dt_m} = 55$ mm, which is much longer than the gas cell length. Therefore, 5 minutes is enough interval time for a 2 cm cell. By decreasing the spacing between the two windows, the time for output stabilization is reduced, i.e. 10 mm spacing only requires 0.1 s.

SEIRA with MHAs has the potential to detect gases in thin gas cells since it is linked to optical near-field enhancement. Use of the cavity effect could open new possibilities for miniaturization and will be investigated next. The detector used in this study has 100-200 nm wide IR-bandpass filter windows which can be substituted with MHAs and integrated into the gas cell, reducing the overall setup costs. Optimization of gas cell thickness and introduction of a larger absorbing MHA surface are expected to further increase sensitivity into the 1-10 ppm (40-400 nM) range (see the changes introduced by one MHA window in Fig. 4(b)). Simple focusing of IR light transmitted through the gas cell by a cylindrical lens onto the IR detector should yield extra sensitivity and lower detection threshold.

4.2. Numerical simulations of transmission of MHA

The transmission and field enhancement properties of the gas cell were simulated with 3D-FDTD. The mirrors were modeled as silicon slabs supporting a silver layer of thickness t in which the MHA of period $a = 3.3$ μm and hole diameter $c = a/2$ is realized, as shown in Fig. 5(a). The refractive index spectra of the materials are fitted from the experimental values obtained in literature, by means of a built-in polynomial model. In order to reduce the computational demands, only a 13.2×17.15 μm^2 section of the mirror pair is modeled, as shown by the box in Fig. 5(a), and the distance between the mirrors is reduced to 10 μm. The *x*- and *y*-direction boundaries are closed by periodic boundary conditions (PBCs) to extend the lattice indefinitely. The cell is illuminated by a linearly *x*-polarized plane wave source with bandwidth extending from 9 to 13 μm wavelength, and the domain is closed in the *z*-direction by perfectly-matched layers (PMLs) to avoid reflections. The transmitted and reflected power are sampled by monitors at both domain ends, and the cell is tested for different values of thickness of the MHA layer $t = 20, 50, 100$ nm.

The results are shown in Fig. 5(b), where the power values are normalized to source power. It can be noticed that the thinner layer has a broader transmission bandwidth around 10 and 11 μm, whose upper limit is reduced down to 10.7 μm by thickening the layer. Conversely, the average transmission increases from around 80% to 90%, much higher than the experiment due to the smaller optical path of the simulated device and absence of the gas cell between the mirrors. It is interesting to look at the local E-field intensity enhancement around the MHA holes at the characteristic wavelength of 10.6 μm, which is shown as the *xz*-plane cross-section in Fig. 5(c) for $t = 100$ nm and in Fig. 5(d) for $t = 20$ nm. In the thicker case, it can be seen that there is sign of extraordinary transmission into the air from the silicon side of the array

#187633 - $15.00 USD Received 25 Mar 2013; revised 26 May 2013; accepted 29 May 2013; published 13 Jun 2013

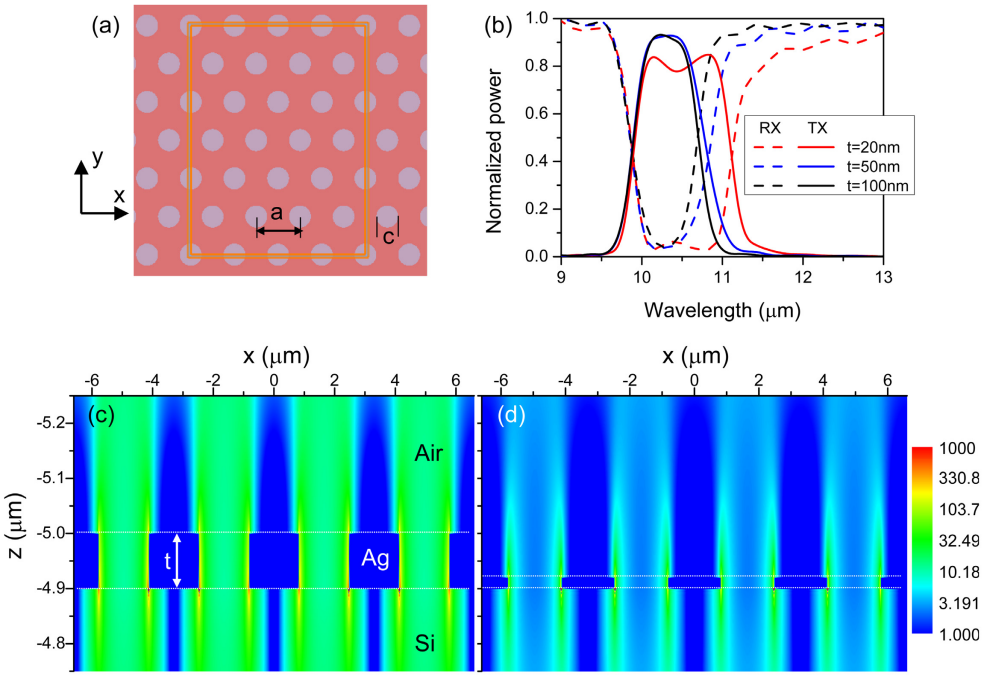

Fig. 5. (a) Simulation layout of the Ag MHA of period $a = 3.3$ μm and hole diameter $c = a/2$, the box indicates the footprint of the elementary simulation cell, made periodic through the boundaries. (b) Normalized power reflected (RX) and transmitted (TX) out of a 10-μm long gas cell realized with Si:MHA mirrors as in the black inset of Fig. 4(a), for different thickness t of the Ag MHA. (c) xz-plane cross-section of a Si:MHA mirror with $t = 100$ nm illuminated from bottom, depicting E-field intensity enhancement at 10.6 μm wavelength; (d) same for $t = 20$ nm.

(illumination is from bottom), so that the green-colored region (enhancement greater than 10) extends for 250 nm and more beyond the MHA, accounting for greater gas cell transmission. In the thinner case, the enhancement is weaker and the high-enhancement region fades out within 100 nm beyond the MHA. The maximum calculated intensity enhancement at the silver-silicon interface was 16000 for $t = 100$ nm, and 4000 for $t = 20$ nm.

5. Conclusion

In this study, we demonstrate SEIRA with MHAs for gas sensing. With the MHA, absorption increased 27 times for a detection threshold around 5 ppm in the current setup with two Si:MHA mirrors, using a simple $\sim$ \$200 dollars detector. This plasmonic gas sensor has potential in a multi-layer plasmonic device, where high-transparency plates are stacked into the path of a IR-light beam and strong electromagnetic field enhancement on larger areas would deliver higher sensitivity. It can also be implemented in a microfluidic Fabry-Pérot geometry [18, 19] or used in gas concentrators by a micro-jet [19]. The same principle can be applied not only for the SF_6 gas, but also for any other molecules with distinct IR active vibrational modes in near-IR and far-IR. It is promising for bio-/medical and security applications. Here we show how the sensitivity of NDIR measurements can benefit from plasmonic effects already utilized in surface-enhanced Raman sensing of explosive precursors in gas phase [20].

#187633 - \$15.00 USD Received 25 Mar 2013; revised 26 May 2013; accepted 29 May 2013; published 13 Jun 2013

Acknowledgments

The authors are grateful to Prof. T. Baba from Yokohama Nat. Univ. for fruitful discussions and for granting access to the fabrication facilities. We thank Tokyo Ohka Kogyo Co. Ltd. for providing the photoresist and surfactant used for fabrication, and the Instrumental Analysis Center (Yokohama Nat. Univ.) for the FTIR in fabrication of MHA. This work was financially supported by the Nippon Sheet Glass Foundation for Materials Science and Engineering (NSG Foundation), Research Foundation for opt-Science and Technology, and Amada Foundation. SJ is grateful for support via the Australian Research Council DP130101205 Discovery project. Part of this work was performed on the swinSTAR supercomputer at Swinburne University of Technology.

#187633 - $15.00 USD Received 25 Mar 2013; revised 26 May 2013; accepted 29 May 2013; published 13 Jun 2013